JPE 18-1-19

https://doi.org/10.6113/JPE.2018.18.1.204
ISSN(Print): 1598-2092 / ISSN(Online): 2093-4718

Frequency and Voltage Control Strategies of the Jeju Island Power System Based on MMC-HVDC Systems

Ngoc-Thinh Quach*, Sang Heon Chae*, Seung-Ho Song**, and Eel-Hwan Kim†

*,†Department of Electrical Engineering, Jeju National University, Jeju, Korea
**Department of Electrical Engineering, Kwangwoon University, Seoul, Korea

Abstract

At present, one of two LCC-HVDC systems is responsible for controlling the grid frequency of the Jeju Island Power System (JIPS). The grid voltage is regulated by using STATCOMs. However, these two objectives can be achieved in one device that is called by a modular multilevel converter-high voltage direct current (MMC-HVDC) system. Therefore, this paper proposes frequency and voltage control strategies for the JIPS based on a MMC-HVDC system. In this case, the ancillary frequency and voltage controllers are implemented into the MMC-HVDC system. The modelling of the JIPS is done based on the parameters and measured data from the real JIPS. The simulation results obtained from the PSCAD/EMTDC simulation program are confirmed by comparing them to measured data from the real JIPS. Then, the effect of the MMC-HVDC system on the JIPS will be tested in many cases of operation when the JIPS operates with and without STATCOMs. The objective is to demonstrate the effectiveness of the proposed control strategy.

Key words: Frequency control, Jeju island power system, LCC-HVDC, MMC-HVDC, STATCOM, Voltage control

I. INTRODUCTION

Jeju Island has the best conditions for wind power generation because it has the highest average wind speed (about 7~8m/s) among all of the promising sites in South Korea [1], [2]. Thus, the local government of Jeju Island has a plan, namely the "Carbon Free Island Jeju by 2030". To carry out this plan, the total installed capacity of wind farms will need to be increased up to 1.09 GW by 2020 [3]. At that time, the wind farms will be able to supply about 500 MW of active power to the Jeju Island Power System (JIPS) among the 944 MW load demand. Consequently, the JIPS may become unstable because the JIPS is a weak grid that consists of two line-commutated converter-high voltage direct current (LCC-HVDC) systems, thermal power plants, wind farms, two static synchronous compensators (STATCOMs) and electric loads. In order to stabilize the JIPS, a new HVDC system, which serves as a link between the mainland power system and the JIPS, will be installed in the near future. In addition, to transfer the active power from wind farms to the JIPS, a HVDC system is also a good choice [4]-[6]. Recently, a modular multilevel converter (MMC) has emerged as a promising voltage source converter topology. The operation of MMC-HVDC systems have been investigated by many authors around the world [7]-[10]. The MMC is a type of voltage source converter (VSC). It has many advantages over the conventional converter topologies such as a low total harmonic distortion, low switching frequency, high capacity and high availability. Therefore, a MMC-HVDC system is recommended for the JIPS in order to connect between the mainland power system and the JIPS, and between wind farms and the JIPS. The application of a MMC-HVDC system that connects between the mainland power system and the JIPS has been researched in [11], [12]. In these papers, the authors analyzed the balancing of the active power flow and the ability to regulate grid voltage with a MMC-HVDC system in the JIPS. However, the ability to regulate the grid frequency with a MMC-HVDC system has not been studied

Manuscript received Mar. 22, 2017; accepted Aug. 12, 2017
Recommended for publication by Associate Editor Kyeon Hur.
†Corresponding Author: ehkim@jejunu.ac.kr
Tel: +82-64-754-3674, Fax: +82-64-756-5281, Jeju National University
*Department of Electrical Engineering, Jeju National University, Korea
**Department of Electrical Engineering, Kwangwoon University, Korea

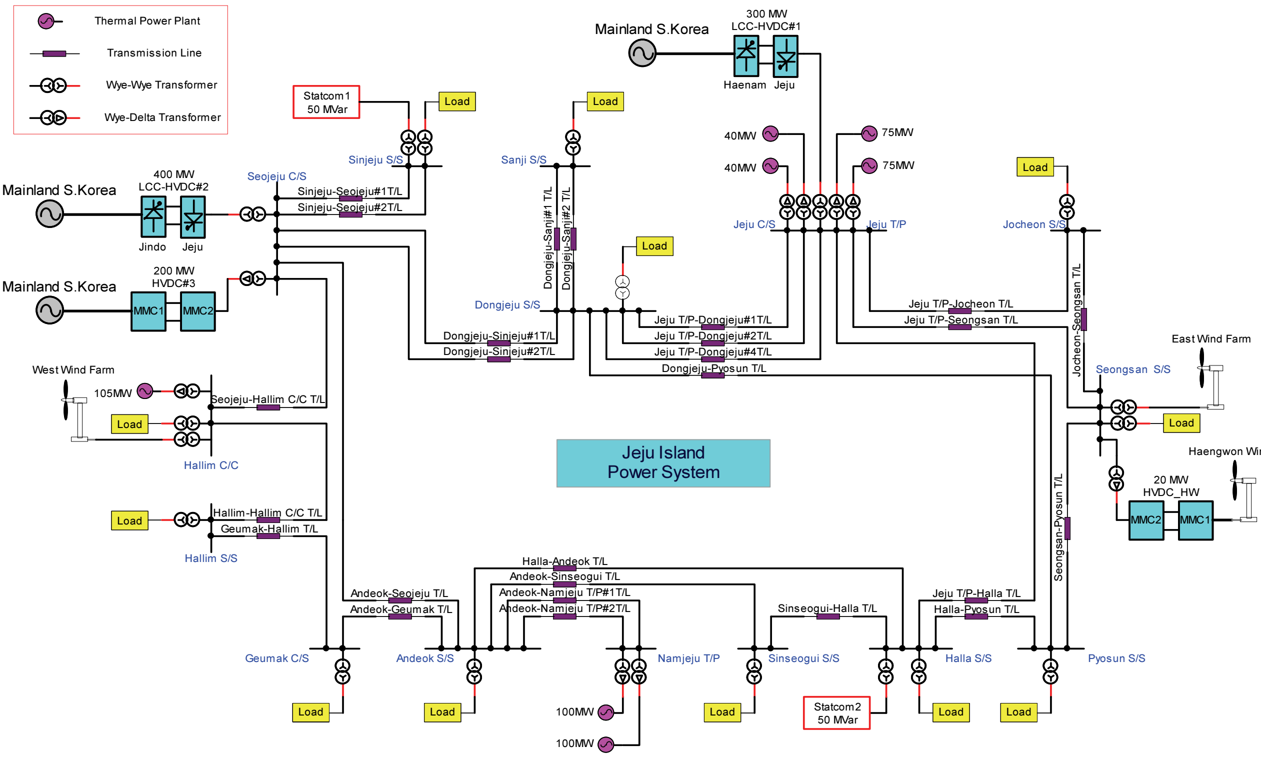

Fig. 1. Configuration of the Jeju Island power system.

yet. The application of a MMC-HVDC system to wind farms has been presented in [13], [14]. With the appearance of MMC-HVDC systems, the operating strategies of the JIPS should be changed. Therefore, this paper proposes frequency and voltage control strategies for the JIPS based on a MMC-HVDC system. In this case, ancillary frequency and voltage controllers are implemented into the MMC-HVDC system. First, modelling of the JIPS is confirmed by comparing simulation results to measured data from the real JIPS. Then, the operation of the JIPS is tested in specific cases when the JIPS operates with and without using STATCOMs.

The rest of this paper is organized as follows. Section II shows the configuration of the JIPS. The proposed control strategies are explained in Section III. Section IV presents simulation results and discussion. Section V draws some conclusions.

II. Configuration of the Jeju Island Power System

The future configuration of the JIPS is shown in Fig. 1. At present, the JIPS consists of two LCC-HVDC systems, two STATCOM systems, wind farms, thermal power plants, transformers, transmission and distribution lines, and a load. The total installed capacity of the wind farms is about 114.645 MW. Because the output power of the wind farms is not stable, the thermal power plants and the LCC-HVDC systems generate both active and reactive powers in order to support the power system. However, the reactive power of the LCC-HVDC systems is related to the active power strictly (it is about 60% of the active power), and is almost constant. Because of the dependence of reactive power on active power, the reactive power generated from the LCC-HVDC systems is often higher than the demand for reactive power. This causes an over voltage phenomenon in the power system. To solve this problem, two STATCOMs have been installed at the Sinjeju and Halla sub-stations in order to regulate the grid voltage. The local government of Jeju Island has a plan, namely the “Carbon Free Island Jeju by 2030”. From this plan, the total capacity of wind farms will increase up to 1.09 GW by 2020. With this increase of wind power, a new 200 MW MMC-HVDC transmission system, HVDC#3, will be installed in the future in order to exchange active power between the JIPS and the mainland power system. In addition, to connect between the wind farms and the JIPS, the MMC-HVDC system will also be a good choice. The first MMC-HVDC system, HVDC_HW, will be installed at the Haengwon wind farm with a capacity of 20 MW. In other words, the future JIPS is developed on the basic of the present JIPS with the implementation of HVDC#3 and HVDC_HW.

The wind farms, thermal power plants, LCC-HVDC#1, and LCC-HVDC#2 supply electric power to the load. This means that they inject a three-phase current into the power system. Thus, the wind farms, thermal power plants, LCC-HVDC#1, and LCC-HVDC#2 can be modelled by a controlled-current source. Fig. 2 shows a modelling of the Jeju thermal power plant in the PSCAD/EMTDC simulation program. The other models are similar.

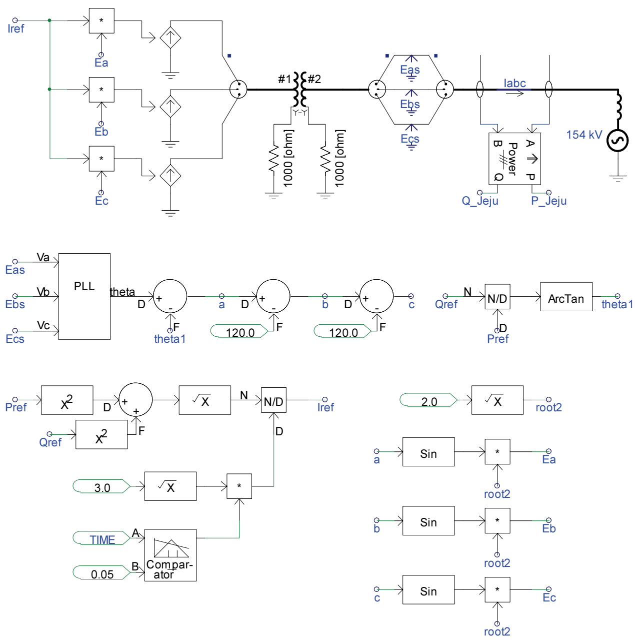

Fig. 2. Modelling of the Jeju thermal power plant.

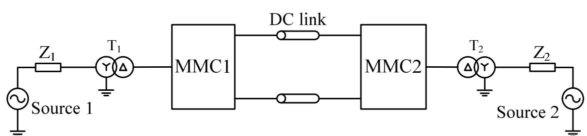

Fig. 3. Configuration of a MMC-HVDC system.

III. Proposed Control Strategies

A. MMC-HVDC System

The configuration of a MMC-HVDC system is shown in Fig. 3. It consists of two MMCs connected back-to-back. The AC side of the MMC is linked to the utility grid via a Y- Δ transformer. The MMC is created by six arms as can be seen in Fig. 4(a). Each arm is made up of *N* submodules (SMs) connected in series and a series arm inductor. The structure of the SM is illustrated in Fig. 4(b). Because a MMC is a type of VSC, it has the ability to control the active power and the reactive power, independently. Normally, one MMC is used to control the active power and reactive power; while the other MMC is responsible for controlling the DC-link voltage and reactive power. The controller of the MMC-HVDC system is shown in Fig. 5.

+ If $S_a = a_1$, the MMC controls the active power and reactive power.

+ If $S_a = a_2$, the MMC controls the DC-link voltage and the reactive power.

B. Frequency Control

In a power system, if the active power flow is unbalanced, the rotor speed of the generator will be significantly affected. Consequently, the frequency of the power system is deviated from its nominal value. At present, the regulation of the

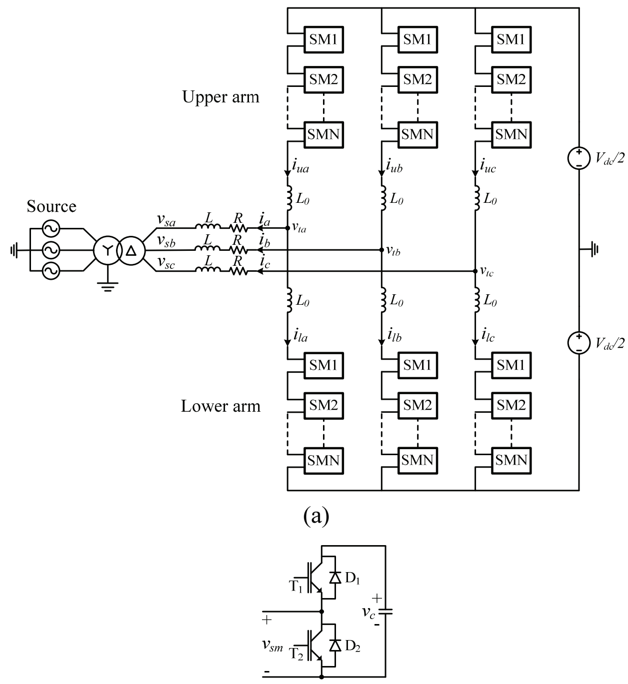

(a)

(b)

Fig. 4. Circuit diagram of a MMC system: (a) circuit diagram; (b) submodules.

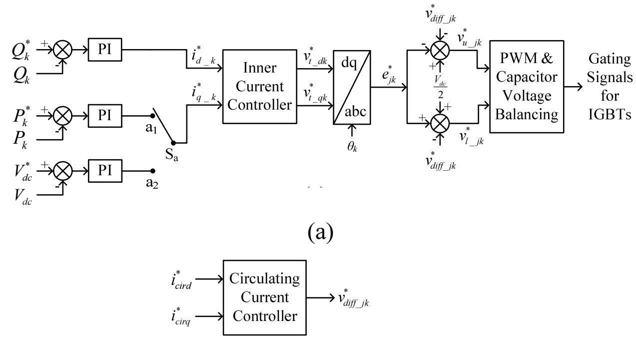

(a)

(b)

Fig. 5. Control diagram of a MMC-HVDC system: (a) main controller; (b) circulating current controller.

frequency in the JIPS belongs to the thermal power plants and LCC-HVDC#1. However, the use of thermal power plants is limited in the future because Jeju Island will become a carbon free island. With an increasing of the load demand, LCC-HVDC#1 and LCC-HVDC#2 will be operated as constant power sources. This is to avoid fluctuations of the reactive power in the power system because the reactive powers of LCC-HVDC#1 and LCC-HVDC#2 depend on the active powers. Therefore, HVDC#3 will be responsible for controlling the frequency of the JIPS.

Normally, the q-axis current controller of a MMC-HVDC system can be expressed as:

$$i_{q\_k}^{*} = \left(k_p + \frac{k_i}{s}\right)\left(P_k^{*} - P_k\right) \quad (1)$$

where *k* denotes MMC1 and MMC2, *k* = 1, 2. * expresses the reference value. i_{q_k} is the q-axis current component. P_k is the active power of MMCk. k_p and k_i are the gains of the PI controller.

Once an ancillary frequency controller is implemented into the MMC-HVDC system, the current controller will be:

$$i^*_{q\_k} = \left(k_p + \frac{k_i}{s}\right)\left(P^*_k + P^*_{kf} - P_k\right) \quad (2)$$

Where $$P^*_{kf} = \left(k_p + \frac{k_i}{s}\right)\left(f^*_k - f_k\right) \quad (3)$$

f_k is the frequency at the MMCk side. P^*_{kf} denotes the compensation power for the frequency control.

If the system frequency drops lower than the nominal frequency, the compensation power, P^*_{kf}, becomes positive. This means that the active power demand of the JIPS is higher than the active power generation. Thus, the JIPS needs a lot more active power from the mainland power system. If the system frequency increases higher than the nominal frequency, the compensation power becomes negative. The MMC-HVDC system must reduce the active power that is transferred from the mainland power system to the JIPS. The frequency controller is shown in Fig. 6.

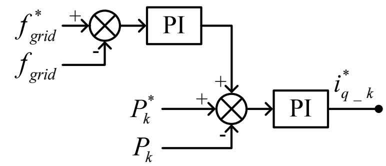

Fig. 6. Frequency controller.

C. Voltage Control

The MMC is a type of VSC. Thus, it can control the active power and the reactive power, independently. In addition, it has been demonstrated that the MMC-HVDC system has ability to generate or consume reactive power. Based on these characteristics, the MMC-HVDC system is also designed to support the grid voltage via control of the reactive power.

The d-axis current controller of a MMC-HVDC system is expressed as:

$$i^*_{d\_k} = \left(k_p + \frac{k_i}{s}\right)\left(Q^*_k - Q_k\right) \quad (4)$$

where i_{d_k} is the d-axis current component. Q_k is the reactive power of MMCk.

The reference reactive power can be achieved from the voltage controller as:

$$Q^*_k = \left(k_p + \frac{k_i}{s}\right)\left(V^*_{grid} - V_{grid}\right) \quad (5)$$

where V_{grid} is the grid voltage.

The voltage controller is shown in Fig. 7. Moreover, with the installation of a MMC-HVDC system for connecting between the Haengwon wind farm and the JIPS, a coordinated reactive power control can be used in order to support the grid voltage. In this strategy, HVDC#3 regulates the grid voltage at the Seojeju C/S while HVDC_HW regulates the grid voltage at the Seongsan S/S.

In this paper, the controls of HVDC#3 and HVDC_HW are as follows.

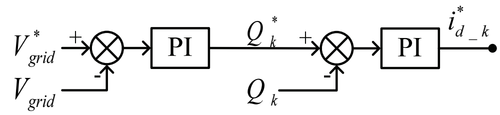

Fig. 7. Voltage controller.

TABLE I
SIMULATION CASES

Component	Case 1	Case 2	Case 3	Case 4
LCC-HVDC#1	x	-	-	x
LCC-HVDC#2	x	x	x	x
HVDC#3	-	x	x	x
HVDC_HW	-	-	-	x
STATCOM1	x	x	-	-
STATCOM2	x	x	-	-
Thermal power plants	x	x	x	x
Wind farms	x	x	x	x

- HVDC#3:
+ MMC1 controls the DC-link voltage and the reactive power.
+ MMC2 controls the active power, the frequency and the grid voltage.
- HVDC_HW:
+ MMC1 controls the active power and the reactive power.
+ MMC2 control the DC-link voltage and the grid voltage.

IV. SIMULATION RESULTS AND DISCUSSION

The simulation cases are summarized in Table I. HVDC#3 is a MMC-HVDC system which is used to connect between the mainland power system and the JIPS. HVDC_HW is also a MMC-HVDC system which transfers active power from the Haengwon wind farm to the JIPS. The modelling of the JIPS is performed by using the PSCAD/EMTDC simulation program. In the simulation, the powers are measured at the output side of each component. The grid voltage and frequency are measured at the Seojeju C/S.

In Table I, the symbol "x" means that the component is available in operation.

In the figures, the symbols should be noted as follows.
+ P_HVDC1: the active power of LCC-HVDC#1.
+ P_HVDC2: the active power of LCC-HVDC#2.
+ P_HVDC3: the active power of HVDC#3 (MMC-HVDC).
+ P_TPP: the total active power generated by the thermal power plants.

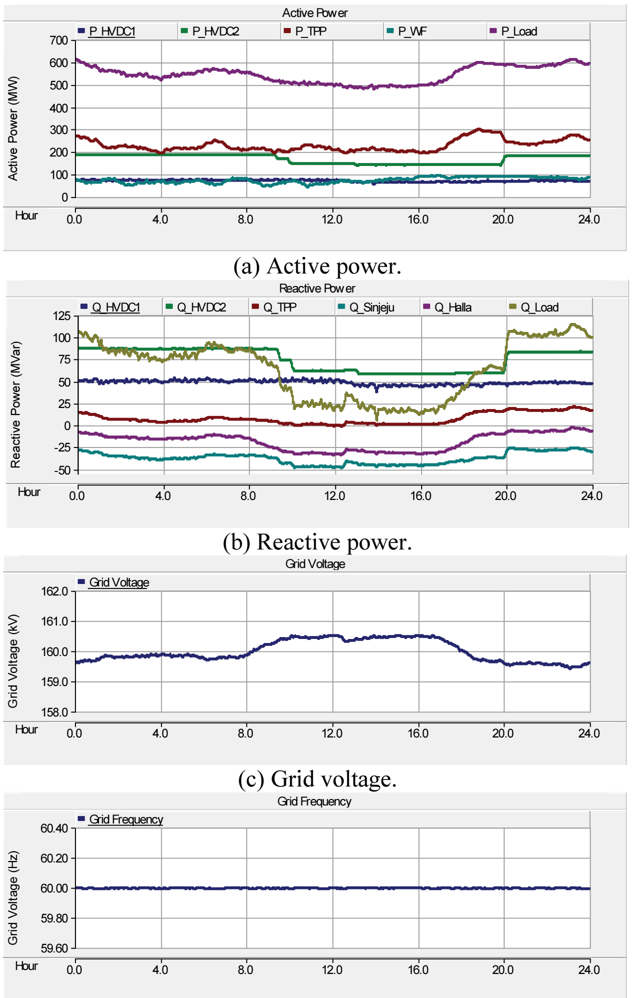

(a) Active power.

(b) Reactive power.

(c) Grid voltage.

(d) Grid frequency.

Fig. 8. Measured data from the real Jeju Island power system on Feb. 28, 2015.

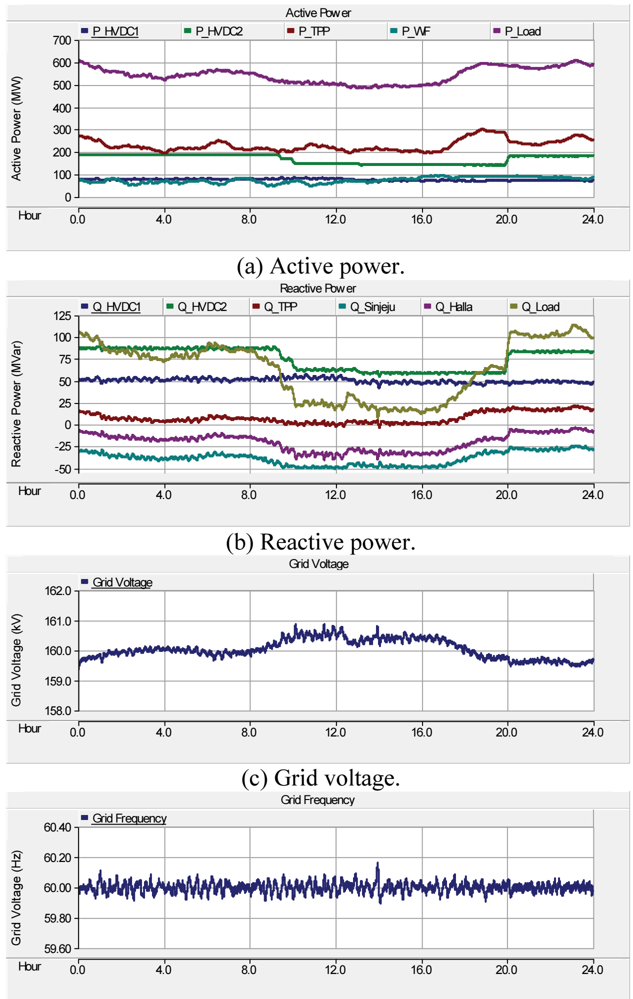

(a) Active power.

(b) Reactive power.

(c) Grid voltage.

(d) Grid frequency.

Fig. 9. Simulation results of the Jeju Island power system.

+ P_WF: the total active power generated by the wind farms.

+ P_Load: the demand for active power.

+ Q_HVDC1: the reactive power of LCC-HVDC#1.

+ Q_HVDC2: the reactive power of LCC-HVDC#2.

+ Q_HVDC3: the reactive power of HVDC#3 (MMC-HVDC).

+ Q_TPP: the total reactive power generated by the thermal power plants.

+ Q_Sinjeju: the reactive power of the STATCOM at the Sinjeju S/S.

+ Q_Halla: the reactive power of the STATCOM at the Halla S/S.

+ Q_Load: the demand for reactive power.

A. Case 1

The modelling of the JIPS is confirmed by comparing the simulation results to the measured data from the real JIPS on Feb. 28, 2015, as shown in Fig. 8 and Fig. 9. It can be seen that the measured data and the simulation results are similar. This demonstrates the exactness of the modelling of the JIPS. LCC-HVDC#1 and LCC-HVDC#2 nearly supply the constant active and reactive powers as can be seen in Figs. 8(a)-(b) and Figs. 9(a)-(b). With the LCC-HVDC system, the reactive power always depends on the active power. An increase or decrease in the active power of the LCC-HVDC system leads to an increase or decrease in the reactive power. Consequently, while the total active power generated from LCC-HVDC#1, LCC-HVDC#2, the thermal power plants and the wind farms match the demand for active power well, the total reactive power generated from LCC-HVDC#1, LCC-HVDC#2 and the thermal power plant is higher than the demand for reactive power. Therefore, two STATCOMs always consume the reactive power during the operating time to balance the power flow on the JIPS. As a result, the grid voltage and grid frequency are stable around their nominal values as shown in Figs. 8(c)-(d) and Figs. 9(c)-(d).

B. Case 2

LCC-HVDC#1 is replaced by HVDC#3 in order to verify the operation of the HVDC#3 system. Due to the increase in the wind power generation and load demand, HVDC#3 will

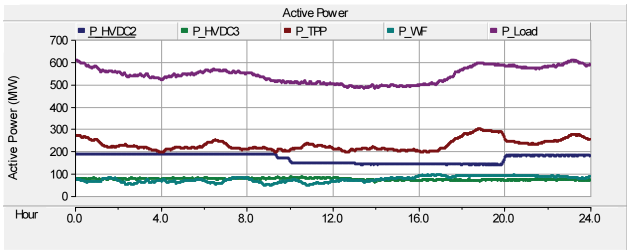

(a) Active power.

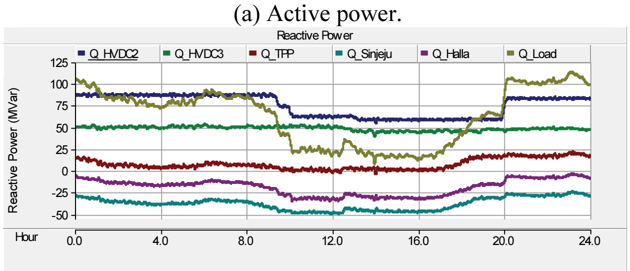

(b) Reactive power.

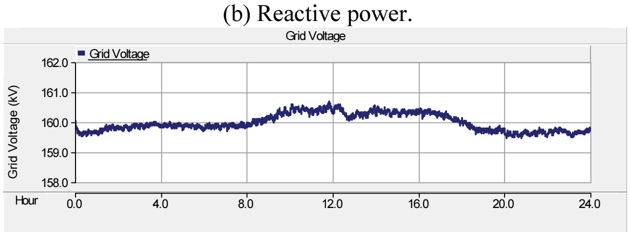

(c) Grid voltage.

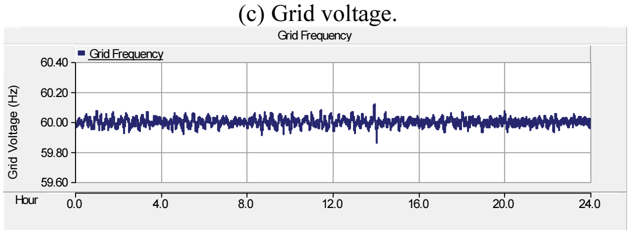

(d) Grid frequency.

Fig. 10. Operation of the Jeju Island power system with HVDC#3 and STATCOMs.

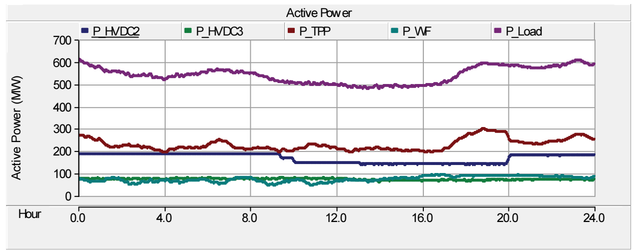

(a) Active power.

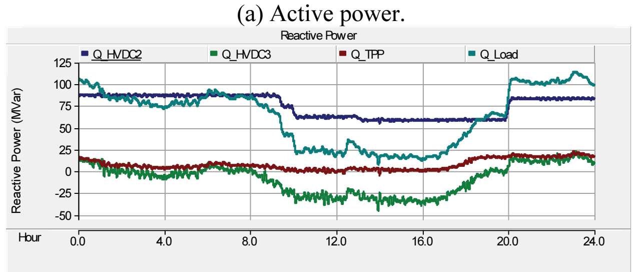

(b) Reactive power.

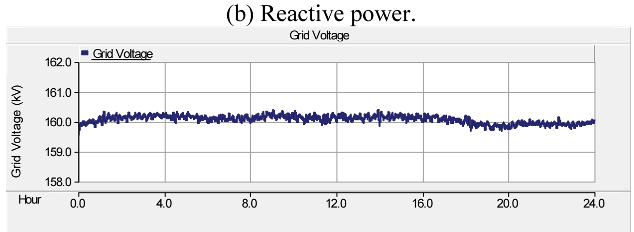

(c) Grid voltage.

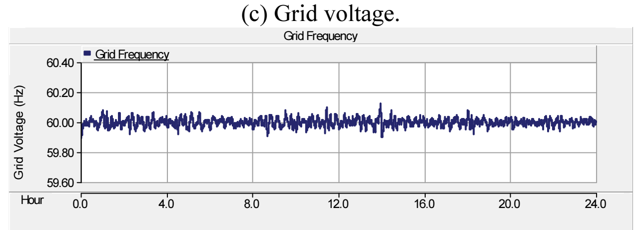

(d) Grid frequency.

Fig. 11. Operation of the Jeju Island power system with HVDC#3 and without STATCOMs.

be installed in the near future. The operation of the JIPS with HVDC#3 is shown in Fig. 10. It is clear that the simulation results have a good agreement with the measured data in Fig. 8. Thus, the modelling of the JIPS with HVDC#3 is confirmed. HVDC#3 can regulate the grid frequency by using an ancillary frequency controller that has the same function as LCC-HVDC#1. In this case, the MMC-HVDC replaces the function of LCC-HVDC#1 and reduces harmonics.

C. *Case 3*

LCC-HVDC#1 is replaced by HVDC#3. Then, the JIPS operates without using two STATCOMs. This is derived from the operation of STATCOMs as explained in Section 4.A. The STATCOMs consume the surplus reactive power of the JIPS. Meanwhile, the MMC-HVDC system, HVDC#3, can consume or generate the reactive power like a STATCOM. Therefore, it can replace the function of the STATCOM. In this case, the active powers are the same as Case 2 as shown in Fig. 11(a). With the ancillary voltage controller, HVDC#3 regulates the grid voltage via the reactive power control as can be seen in Fig. 11(b). Without using two STATCOMs, the power flow on the JIPS is still balanced. Thus, the grid voltage and grid frequency are stable during the operating time as illustrated in Figs. 11(c)-(d). With the appearance of HVDC#3, the usage of STATCOMs is not necessary. The STATCOMs can operate as standby systems for HVDC#3. This can reduce both the operating and maintenance costs.

D. *Case 4*

From the above analysis, the modelling of the JIPS and the ability to control the grid frequency and grid voltage of the MMC-HVDC system have been confirmed. This section is to explain the operation of the future JIPS. In this study, the HVDC_HW is only implemented an ancillary voltage control, while HVDC#3 is implemented both ancillary voltage and frequency controllers. Then, the JIPS operates with LCC-HVDC#1, LCC-HVDC#2, HVDC#3, HVDC_HW, and without two STATCOMs. The operations of HVDC#3 and HVDC_HW are shown in Fig. 12 and Fig. 13, respectively. Although the active power and reactive power are variable, the DC-link voltages of the two MMC-HVDC

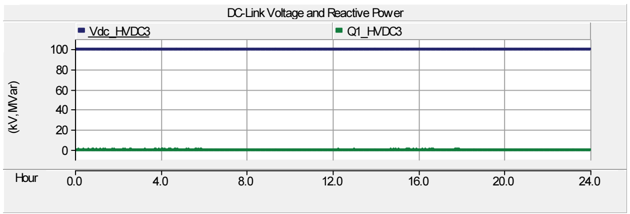

(a) DC-Link voltage and reactive power.

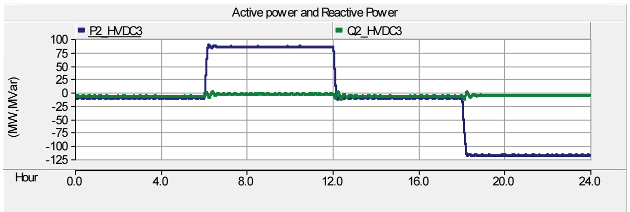

(b) Active power and reactive power.

Fig. 12. Operation of HVDC#3.

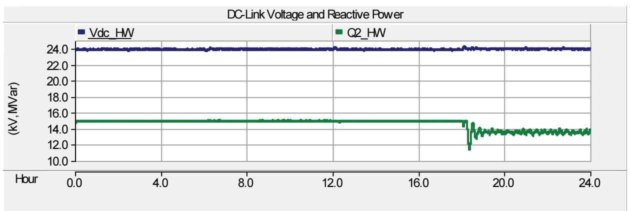

(a) DC-Link voltage and reactive power.

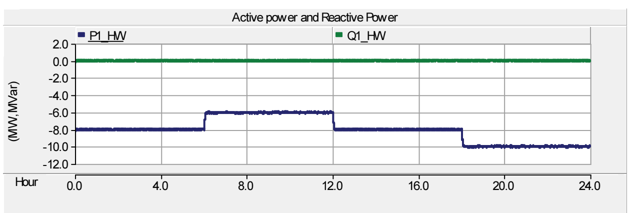

(b) Active power and reactive power.

Fig. 13. Operation of HVDC_HW.

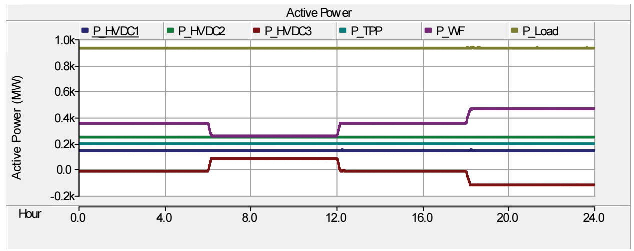

(a) Active power.

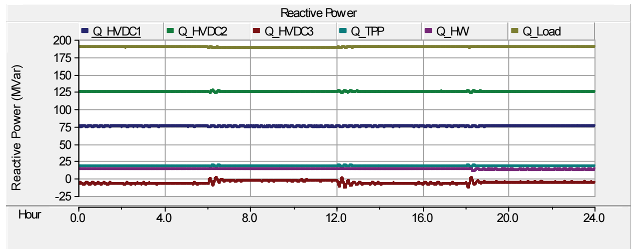

(b) Reactive power.

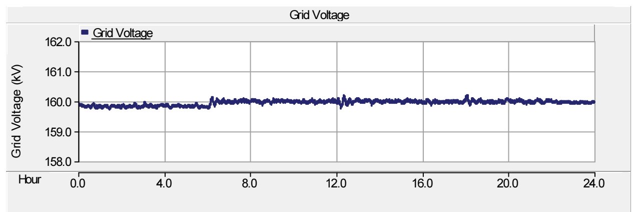

(c) Grid voltage.

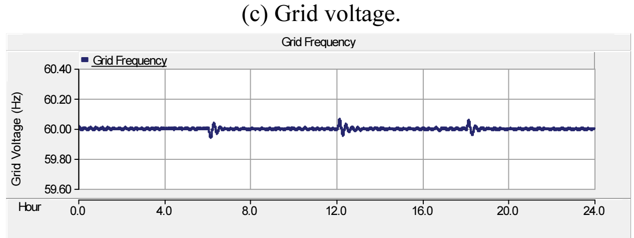

(d) Grid frequency.

Fig. 14. Operation of the future Jeju Island power system.

systems are almost unchanged during the simulation time. This demonstrates the reliability of the proposed MMC-HVDC systems. The operation of the future JIPS is shown in Fig. 14. The active powers and total load demand are expressed in Fig. 14(a). The output power of the wind farm is changed at t = 6s, t = 12s and t = 18s in order to verify the dynamic response of HVDC#3 and HVDC_HW. In this case, the frequency controller of HVDC#3 is responsible for balancing the active power flow in the JIPS. The main reactive power sources are generated from LCC-HVDC#1, LCC-HVDC#2 and the thermal power plants as can be seen in Fig. 14(b). With the coordinated reactive power control between HVDC#3 and HVDC_HW, the grid voltage is regulated at around its nominal value. HVDC_HW supplies reactive power to the JIPS (Fig. 13(a)), while HVDC#3 consumes reactive power from the JIPS (Fig. 12(b) or Fig. 14(b)). Because of the excellent response of the MMC-HVDC systems, the active power and reactive power in the JIPS are balanced. Thus, the grid voltage and grid frequency are stable around their nominal values as shown in Figs. 14(c)-(d).

V. CONCLUSIONS

This paper has proposed frequency and voltage control strategies for the JIPS based on the MMC-HVDC system. The modelling of the JIPS has been confirmed by comparing simulation results to measured data from the real JIPS on Feb. 28, 2015. From this point, the ability to control the grid voltage and frequency of HVDC#3 has been demonstrated by implementing both ancillary voltage and frequency controllers into the MMC-HVDC system. With HVDC#3, HVDC_HW and the proposed control strategies, the power flows in the future JIPS are still balanced. Consequently, the grid voltage and frequency of the JIPS are stable around their nominal values. In addition, the use of STATCOMs is not necessary because the MMC-HVDC system can replace the function of STATCOMs. Therefore, the operation cost and maintenance cost can be reduced.

ACKNOWLEDGMENT

This work was supported by the Development of 20MW VSC HVDC for offshore wind-farm interconnection of the Korea Institute of Energy Technology Evaluation and Planning (KETEP), granted financial resource from the Ministry of Trade, Industry & Energy, Republic of Korea. (No. 2012T100201551).

This work was supported by the Korea Institute of Energy Technology Evaluation and Planning (KETEP) and the Ministry of Trade, Industry & Energy (MOTIE) of the Republic of Korea (No. 20173010024890).

REFERENCES

[1] E.-H. Kim, J.-H. Kim, S.-H. Kim, J. Choi, K.Y. Lee, and H.-C. Kim, "Impact analysis of wind farms in the Jeju island power system," *IEEE Syst. J.*, Vol. 6, No. 1, pp. 134-139, Mar. 2012.

[2] F. Zhang, K. Cho, J. Choi, Y.-M. Lee, and K. Y. Lee, "A study on wind speed prediction using artificial neural network at Jeju island in Korea II," *2011 IEEE 54th International Midwest Symposium on Circuits and Systems (MWSCAS), Seoul, South Korea*, pp. 1-4, 2011.

[3] Jeju Special Self-Governing Province, Policy report, Carbon free island Jeju by 2030, May 2012.

[4] S. M. Muyeen, R. Takahashi, and J. Tamura, "Operation and control of HVDC-connected offshore wind farm," *IEEE Trans. Sustain. Energy*, Vol. 1, No. 1, pp. 30-37, Apr. 2010.

[5] H. Liu and Z. Chen, "Contribution of VSC-HVDC to frequency regulation of power systems with offshore wind generation," *IEEE Trans. Energy Convers.*, Vol. 30, No. 3, pp. 918-926, Sep. 2015.

[6] D. Elliott, K. R. W. Bell, S. J. Finney, R. Adapa, C. Brozio, J. Yu, and K. Hussain, "A comparison of AC and HVDC options for the connection of offshore wind generation in Great Britain," *IEEE Trans. Power Del.*, Vol. 31, No. 2, pp. 798-809, Apr. 2016.

[7] M. Saeedifard and R. Iravani, "Dynamic performance of a modular multilevel back-to-back HVDC system," *IEEE Trans. Power Del.*, Vol. 25, No. 4, pp. 2903-2912, Oct. 2010.

[8] Q. Tu, Z. Xu, and L. Xu, "Reduced switching-frequency modulation and circulating current suppression for modular multilevel converters," *IEEE Trans. Power Del.*, Vol. 26, No. 3, pp. 2009-2017, Jul. 2011.

[9] M. Guan and Z. Xu, "Modeling and control of a modular multilevel converter-Based HVDC system under unbalanced grid conditions," *IEEE Trans. Power Electron.*, Vol. 27, No. 12, pp. 4858-4867, Dec. 2012.

[10] N.-T. Quach, J.-H. Ko, D.-W. Kim, and E.-H. Kim, "An application of proportional-resonant controller in MMC-HVDC system under unbalanced voltage conditions," *J. Electr. Eng. Technol.*, Vol. 9, No. 5, pp. 1746-1752, Sep. 2014.

[11] N.-T. Quach, D.-H. Lee, H.-C. Kim, and E.-H. Kim, "Application of MMC-HVDC system for regulating grid voltage based on Jeju Island power system, *Trans. Korean Inst. Power Electron.*, Vol. 19, No. 6, pp. 494-502, Dec. 2014.

[12] N.-T. Quach, D. H. Lee, H.-C. Kim, and E.-H. Kim, "Analyzing stability of Jeju Island power system with modular multilevel converter based HVDC system, *J. Electr. Eng. Technol.*, Vol. 10, No. 1, pp. 47-55, Jan. 2015.

[13] J. Lyu, X. Cai, and M. Molinas, "Frequency domain stability analysis of MMC-based HVDC for wind farm integration," *IEEE J. Emerg. Sel. Topics Power Electron.*, Vol. 4, No. 1, pp. 141-151, Mar. 2016.

[14] R. Vidal-Albalate, H. Beltran, A. Rolan, E. Belenguer, R. Pena, and R. Blasco-Gimenez, "Analysis of the performance of MMC under fault conditions in HVDC-based offshore wind farms," *IEEE Trans. Power Del.*, Vol. 31, No. 2, pp. 839-847, Apr. 2016.

Ngoc-Thinh Quach received his B.S. degree in Electrical Engineering from Can Tho University, Can Tho City, Vietnam, in 2007; and his M.S. and PhD. degrees in Electrical Engineering from Jeju National University, Jeju City, Korea, in 2012 and 2015, respectively. Since 2015, he has been with the Department of Electrical Engineering, Can Tho University, where he is presently working as a Lecturer. In 2016, he was a Postdoctoral Researcher at Jeju National University. His current research interests include power electronics, renewable energy systems, HVDC systems, and power system stability.

Sang Heon Chae received his B.S. and M.S. degrees in Electrical Engineering from Jeju National University, Jeju City, Korea, in 2015 and 2017, respectively, where he is presently working towards his PhD. degree in the Department of Electrical Engineering. His current research interests include microgrid, Energy Storage Systems (ESS) and power electronics.

Seung-Ho Song received his B.S., M.S. and Ph.D. degrees in Electrical Engineering from Seoul National University, Seoul, Korea, in 1991, 1993 and 1999, respectively. Since 2006, he has been a faculty member in the Department of Electrical Engineering, Kwangwoon University, Seoul, Korea, where he is presently working as a full Professor. His current research interests include electric machine drives and renewable energy conversion.

Eel-Hwan Kim received his B.S., M.S. and Ph.D. degrees in Electrical Engineering from Chung-Ang University, Seoul, Korea, in 1985, 1987 and 1991, respectively. Since 1991, he has been with the Department of Electrical Engineering, Jeju National University, Jeju City, Korea, where he is presently working as a Professor. He was a Visiting Scholar at Ohio State University, Columbus, OH, USA, in 1995; and at the University of Washington, Seattle, WA, USA, in 2004. His current research interests include power electronics and control, drive systems, renewable energy control applications and power quality. He is a Member of KIEE, KIPE and IEEE.